Analysis of the binding selectivity and inhibiting mechanism of chlorogenic acid isomers and their interaction with grass carp endogenous lipase using multi-spectroscopic, inhibition kinetics and modeling methods

Zeru Xu[a]; Hongying Du[a, b]*; Qiongju Cao[a]; Anne Manyande [c]; Shanbai Xiong[a, b]

[a] Key Laboratory of Environment Correlative Dietology, Ministry of Education, College of Food Science and Technology, Huazhong Agricultural University, Wuhan, Hubei, P.R. China

[b] National R & D Branch Center for Conventional Freshwater Fish Processing, Wuhan, Hubei 430070, P.R. China

[c] School of Human and Social Sciences, University of West London, Middlesex TW8 9GA, UK

* Corresponding author

Hongying Du: Email: hydu@mail.hzau.edu.cn

Abstract

Polyphenols have been shown to be effective inhibitors of lipase, but the binding selectivity and mechanism of polyphenol isomers and how they interact with lipase are still not yet clear. In the present study, chlorogenic acid (CGA) isomers, neochlorogenic acid (NCGA) and cryptochlorogenic acid (CCGA) were used to explore the binding selectivity and mechanism of

endogenous lipases for grass carp. The results of the inhibition assay indicated that both NCGA and CCGA have dose-dependent inhibitory effects on the lipase, however the inhibition effect of NCGA is better. Fluorescence spectroscopy analysis ascertained that both NCGA and CCGA formed complexes with lipase at a ratio of 1:1, and NCGA exhibited a stronger quenching effect. Molecular dynamics studies have demonstrated that NCGA has greater impact on the structure of lipase and binds more closely to the lipase. Results provide valuable insight for better understanding the mechanisms underlying small structural changes in polyphenols affecting their molecular interaction with lipase.

Keywords: Lipase Neochlorogenic acid; Cryptochlorogenic acid; Interaction mechanism; Molecular dynamics simulation; Lipase.

1 Introduction

In general, aquatic products are clearly prone to lipid oxidation during storage, as they are rich in polyunsaturated fatty acids such as docosahexaenoic acid (DHA) and eicosapentaenoic acid (EPA)(Cao et al., 2019; Siscovick David et al., 2017). However, lipid oxidation usually results in the production of unpalatable flavour and odour, shortening of shelf life, loss of nutritional value (e.g. loss of polyunsaturated fatty acids, PUFAs) as well as possible production of unhealthy molecules, which eventually causes the decline in seafood quality (Maqsood, Benjakul, & Shahidi, 2013; Secci & Parisi, 2016). Among all types of lipid oxidation (autoxidation, photo-oxidation and enzyme-catalyzed oxidation), enzyme-catalyzed oxidation plays an important role in the biological effects of long-chain n-3 and n-6 fatty acid compounds (EPA, DHA, and AA)(Huang & Ahn, 2019). As matter of fact, lipase plays a vital role in the enzymatic oxidation process, which can catalyze the decomposition and synthesis of long-chain acylglycerols at the lipid-water interface (Cherif & Gargouri, 2009).Therefore, inhibiting lipid oxidation induced by endogenous lipase is increasingly essential for fish or fish products.

It is also well known that plant polyphenols as a representative natural preservative (Olatunde & Benjakul, 2018),shows strong inhibition of lipid oxidation during fish processing and preservation (Ju et al., 2018; Martínez-González et al., 2017; Wang, Kou, Lin, & Shi, 2019). For example, Bonito (Sarda sarda) fillets dipped into green tea and grape seed extracts before being frozen, delayed lipid oxidation of fish fillets (Yerlikaya & Gokoglu, 2010). Bayberry polyphenols notably inhibited the decomposition, discoloration, and oxidation of irradiated raw tuna fillets during storage at 4 °C (Bu et al., 2017). Carnosic acid, procyanidin, quercetin and resveratrol treatments were effective in delaying the lipid oxidation and protein degradation of tilapia fillets

during partial freezing (Wei et al., 2021). A whey protein isolate combined with polyphenol extract from ginger, lemongrass and green tea coating could maintain the quality of Asian sea bass steak by preventing lipid oxidation (Chaijan, Panpipat, Panya, Cheong, & Chaijan, 2020).

In our previous study, chlorogenic acid (CGA) was demonstrated to inhibit lipid oxidation through inhibiting the activity of endogenous lipase in grass carp muscle during cold storage (Cao et al., 2019). Other studies have reported that polyphenols possess different inhibitory capability to the lipase, due to differences in the chemical structure of polyphenols. However, the inhibitory ability of polyphenols which have similar structure or very little difference in chemical structure to lipase is still not yet very clear. In the present study, two kinds of CGA isomers, NCGA and CCGA with small chemical structural differences were used to explore the binding selectivity and mechanism of the interaction between polyphenol isomers and lipase. The molecular structure of NCGA and CCGA is shown in Fig S1. The aim of this study is to identify the difference in inhibitory effects of CGA isomers on grass carp endogenous lipase and the corresponding mechanism. Hopefully, it will contribute to our understanding of the research related to lipid oxidation inhibition in fish or other aquatic products.

2 Materials and methods

2.1 Materials

Neochlorogenic acid (NCGA, purity > 98%) and cryptochlorogenic acid (CCGA, purity > 98%) were provided by Shanghai Yuanye Biological Technology Co., Ltd. (Shanghai, China), while 4-nitrophenyl butyrate (4-NPB) was obtained from Sigma–Aldrich Chemical Co (St. Loius, MO, USA). All reagents and chemicals used were of analytical grade and all aqueous solutions were prepared using deionized water.

2.2 Fish sample preparation

All procedures were approved by the Animal Care and Use Committee of Huazhong Agricultural University and performed in accordance with the Guidelines for Care and Use of Laboratory Animals of Huazhong Agricultural University. Fresh grass carp (3.5 ± 0.5 kg, n = 10) were purchased from a local fish market (Wuhan, Hubei, China). The sampled fish were anaesthetized using MS‐222 (100 mg/L,3-Aminobenzoic acid ethyl ester methanesulfonate, Shanghai yuanye Bio-Technology Co., Ltd, Shanghai, P.R. China) and were unconscious before slaughter. The fish were immediately decapitated and gutted, then the red muscle under the skin was removed, and the white muscle collected, weighed, and mixed for further study.

2.3 Preparation of polyphenol solution

NCGA and CCGA were dissolved in buffer B (50 mM Tris-HCl, pH=8.0, containing 0.5% Tritox X -100, 25 mmol/L NaCl) to prepare 1mg/ml stock solutions respectively. Then the polyphenol stock solutions were kept in a refrigerator at 4 °C for further analysis.

2.4 Extraction of endogenous lipase

The extraction of lipase was completed according to the Smichi method with slight modifications (Smichi, Gargouri, Miled, & Fendri, 2013). Extraction buffer A (25 mM Tris–HCl, 150 mM NaCl, 2 mM benzamidine, pH 8) was added to the fish muscle sample in ten times volume (1:10, *w*/*v*). Fresh tissue was homogenized in a blender (Y-QSJ1, Oidire, German) for 3 × 10 s (4000 rpm). Then the mixture was stirred with a magnetic bar (Thermo, Massachusetts, USA) for 45 min (4 °C), and centrifuged for 20 min (4 °C, 10,000×g). The supernatant was collected, and ammonium sulfate was added (40% of the weight of the supernatant), the mixture was stirred for 45 min at 4 °C to completely dissolve the ammonium sulfate, then centrifuged at 4 °C 10000×*g* for 15 minutes,

before collecting the supernatant. Ammonium sulfate continued to be added to the supernatant to a saturation of 60%, centrifuged at 10000×*g* for 15 min, and the precipitate was again collected. The precipitate was placed into a dialysis bag, and desalted with the pre-Tris-HCl buffer A. The sample was left in the refrigerator for 24 hours, and the buffer A changed every 6 hours.

2.5 Enzyme inhibition assay

The lipase inhibitory activity was evaluated using a slightly modified method (Kuepethkaew, Sangkharak, Benjakul, & Klomklao, 2017). Buffer B (2 mL, 50 mM Tris-HCl, pH=8.0, containing 0.5% Tritox X -100, 25 mmol/L NaCl), fixed concentration of lipase (800μl 0.1mg/mL) and various concentrations of NCGA and CCGA (800μl 0.0-0.6 mg/ml) were incubated at 37 ℃ for 2 min. Then the reaction was started by adding 400 μl of 4-npb substrate solution (dissolved in isopropanol) to the mixture solution, which continued to be incubated for 15 min. The blank control was set with the same volume of buffer B replacing the lipase solution. The absorbance of the sample was measured at 410 nm using a spectrophotometer. The inhibition assay of lipase was analyzed by maintaining the final 4-NPB concentration (3mM) and increasing the lipase concentration (0.025, 0.050, 0.100,0.200, 0.300 mg/mL). The reaction velocity (v, ΔA/min) was measured by adding various concentrations of NCGA and CCGA (0, 0.1, 0.2, 0.3 mg/mL). The inhibition kinetics experiment was measured by keeping the lipase concentration as 0.1mg/mL and varied concentrations of NCGA and CCGA (0.0, 0.045, 0.0885, 0.177 mg/mL), and the reaction velocity (v) was calculated by adding the increase of 4-NPB concentration from 1 to 5mmol/L.

2.6 UV absorption spectrum measurement

The UV absorption spectra of the lipase solution (1mg/mL) containing buffer B (50 mM Tris-HCl, pH=8.0, containing 0.5% Tritox X -100, 25 mmol/L NaCl) and the different concentrations of

polyphenols (0, 10, 20, 30, 40×10^{-6} mol/L) were detected using a UV-2600 spectrophotometer (UNIC, China) ranging from 230 to 450 nm.

2.7 Fluorescence spectra measurements

2.7.1 Spectral scanning

Various concentrations of NCGA and CCGA (final concentration ranging from 0 M to 40.0 × 10^{-6} M, stepped by 5 × 10^{-6} M) were successively added into the lipase solution (0.1mg/mL) and buffer B (50 mM Tris-HCl, pH=8.0, containing 0.5% Tritox X -100, 25 mmol/L NaCl). Both intrinsic and synchronous fluorescence spectra were conducted using a fluorescence spectrometer (F-4500, Hitachi, Japan) at two different temperatures (298 and 310 K).

The fluorescence quenching spectrum parameter settings included: excitation wavelength 280 nm, slit width Ex = Em = 5 nm, voltage 400V, scanning speed 1200 nm/min, scanning wavelength range 290 nm-450 nm. The fluorescence synchronous fluorescence parameter settings were wavelength difference is $\Delta\lambda$ = 15 nm, $\Delta\lambda$ = 60 nm, slit width EX = EM = 5 nm, voltage 400 V, scanning speed 1200nm/ min, scanning range 260 nm-350 nm. All the mixtures were balanced for 30 min before measurement and analyses were carried out in triplicate.

2.7.2 The mechanism of fluorescence quenching and determination of quenching constant

The fluorescence quenching process can be divided into static quenching and dynamic quenching. The dynamic quenching process follows the Stem-Volmer equation

$$F_0/F = 1 + K_q\tau_0[Q] = 1 + K_{sv}[Q] \qquad (1)$$

Where F_0 and F are fluorescence intensities of lipase without and with polyphenols, K_{SV} is the quenching constant ($K_{SV}=K_q\tau_0$), which is determined by the linear regression of a plot of F_0/F versus $[Q]$. K_q is the quenching rate constant of biomolecule, τ_0 is the average lifetime of a fluorescence

molecule without a quenching agent (about $10^{-8}s^{-1}$), and [Q] is the concentration of the quencher.

For static quenching, the relationship between the logarithm quenching intensity and the fluorescence intensity of the lipase can be calculated by the following double-logarithm equation:

$$log[(F_0 - F)/F] = logK_a + nlog[Q] \qquad (2)$$

where K_a is the binding constant and same as Eq. (2), n is the number of binding sites per protein.

2.7.3 Thermodynamic analysis

The entropy change (ΔS), enthalpy change (ΔH) and free energy change (ΔG) were estimated by Van't Hoff equation (Zhang, Zhang, Pan, & Gong, 2016)

$$lnK_a = -\Delta H/RT + \Delta S/T \qquad (3)$$

$$\Delta G = -RTlnK_a = \Delta H - T\Delta S \qquad (4)$$

ΔG is the Gibbs free energy change, ΔH is the enthalpy change, ΔS is the entropy change, and T is the corresponding temperature (298 and 310K), R is the gas constant (8.314 J mol^{-1} K^{-1})

2.8 Circular dichroism (CD) spectra measurements

The circular dichroism (CD) spectra of the lipase and lipase-polyphenol system were recorded using a Jasco-1500 spectrophotometer (JASCO, Japan) in the far-UV region (190-250nm) and a scan rate of 200 nm/min under constant nitrogen flush at room temperature. The fixed concentration of lipase was 0.05 mg/ml, and the final concentration levels of NCGA and CCGA were 0, 20, 40 × 10^{-6} mol/L. They were left in the dark for 30 min after mixing and then used to measure circular dichroism. The secondary structure analysis mode is based on Yang's reference.

2.9 Fourier transform infrared (FT-IR) spectroscopy measurements

The lipase solution (0.1mg/mL) containing relative buffer B (50 mM Tris-HCl, pH=8.0, containing 0.5% Tritox X -100, 25 mmol/L NaCl) and various concentrations of polyphenols (0, 20,

40×10^{-6} mol/L) were lyophilized for measurement. FT-IR spectra of all samples were recorded by a Nicolet470 FT-IR spectrometer (Nicolet, USA). The signals were collected in the range of 4000 to 500 cm^{-1} with 64 scans and 4 cm^{-1} resolutions. Background spectrum was recorded before each sample measurement.

2.10 Particle Size Measurement

The particle size of lipase solution (0.1mg/mL) containing relative buffer B and different concentrations of polyphenols at various concentrations (0, 10, 20, 30, 40×10^{-6} mol/L) were measured by the Malvern Zetasizer Nano ZS (Zetasizer Nano ZS, Malvern Instruments, Worcestershire, UK). All samples were determined, and each group was repeated three times.

2.11 Molecular docking

The interaction between lipase and CGA isomers were simulated through the molecular docking approach performed with Discovery Studio 2016 (BIOVIA, USA). The structures of CGA isomers were available in PubChem (http://pubchem.ncbi.nlm.nih.gov/) and the energy minimization was completed. The crystal structure of the lipase (PDB ID: 1ETH) comes from the Protein Data Bank (http://www. rcsb.org/).

To prepare the protein structure, missing and terminal residues of polypeptide chains were repaired, then all water molecules were removed, before hydrogen atoms were added. The docking of protein and CGA isomers were carried out under the CHARMM force field. The CDOCK module was used and chosen From PDB Site Records to define protein binding sites. The Top Hit and Pose Cluster Radius were set to 10 and 0.5, respectively. The other docking parameters not mentioned were the default. The lipase-NCGA and lipase-CCGA interactions were rendered with 3D and 2D diagrams using Discovery Studio.

2.12 Molecular dynamics simulation

The binding mode of lipase and NCGA and CCGA were analyzed from the perspective of kinetics and thermodynamics, as well as the specific situation of various other information about the conformation of the target-ligand docking over time. The GROMACS 2019 (Khoury, Bhatia, & Floudas, 2014) was used to carry out the molecular dynamics simulation. The topology parameters of lipase were taken from Amber's FF03 (Khoury et al., 2014) force field and were obtained by the PDB2GMX tool in gromacs codes. First, the electrostatic potential of the partial charge of each atom of NCGA and CCGA was calculated using the Gaussian09 code at the B3LYP/6-311G** level, and the RESP (Cieplak, Cornell, Bayly, & Kollman, 1995) charge fitting method was employed using the Antechamber tool in AmberTools. Subsequently, the lipase-NCGA and lipase-CCGA complexes were placed in a solvent environment of simulated normal saline (0.15 M NaCl) at a temperature of 300 K to minimize energy for 1000 steps. The minimized system was then equilibrated in NVT ensemble for 100 ps and followed by another 100 ps in NPT ensemble. Then a total 150 ns production run was carried out with a time step of 2 fs at 300K. Primary coordinate track file. 100 frames of kinetic trajectory files were extracted from the last 10 ns stable kinetic trajectories, and the MM/PBSA (Kongsted & Ryde, 2008) method was used to calculate the binding free energy for this trajectory.

2.13 Statistical analysis

All experiments were performed with values presented as the mean ± standard deviation. Statistical analyses were performed using Microsoft Excel 2019 and SPSS 22.0 (IBM, New York, USA) using one-way ANOVA.

3 Results and discussion

3.1 Inhibitory activities and inhibition kinetics for endogenous enzymes

The inhibitory effects of NCGA and CCGA on lipase activity are shown in Fig. 1a1. The inhibition rate results show that NCGA and CCGA exhibited considerable inhibition rates against lipase in a concentration-dependent manner. The IC50 values for NCGA and CCGA of lipase are 0.647 and 0.677 mg/mL, respectively. The results suggest that both NCGA and CCGA have inhibitory effects on lipase, and NCGA had significantly stronger inhibitory activity for lipase compared with CCGA. For assays of the inhibition of lipase, the kinetic plots of the lipase in the presence of different concentrations of NCGA and CCGA were constructed to elucidate the effects. All straight lines pass through the origin with the addition of different amounts of lipase to the reaction system, and the slope decreased with the increase of chlorogenic acid concentration (Fig. 1b1 and 1b2), indicating that the inhibitory effect of NCGA and CCGA on lipase activity is reversible (Yu, Fan, & Duan, 2019). Furthermore, the Lineweaver-Burk plots were measured to evaluate the inhibition type of lipase in the presence of NCGA and CCGA. (Fig. 1c1 and 1c2). For CCGA, the Km value improved with the increase of the cryptochlorogenic acid concentration (from 1.04 mg/mL to 1.40 mg/mL), and the Vm value was constant (0.20 /min), thus CCGA competitively inhibits lipase activity by binding to the active site of endogenous lipase in grass carp muscle. The free enzyme inhibition constant (Ki) was 0.52 mg/mL. For the NCGA inhibition measurement, the addition of NCGA increased the Km value (from 0.98 mg/mL to 1.59 mg/mL), but the Vm (0.15/min) remained constant. The inhibitory type of scutellarin and tea saponin on pancreatic lipase had also a competitive inhibitory effect (Yu et al., 2019).

3.2 Fluorescence Spectra Analysis

3.2.1 Effect of Polyphenols on endogenous enzymes

NCGA and CCGA had significant inhibitory activity on the lipase, which suggests that polyphenols might bind to the lipase directly. However, the detailed binding characteristic is not very clear. In order to further clarify the interaction mode between polyphenols and lipase, fluorescence analysis was carried out.

Fluorescence quenching can be used to evaluate the interaction between protein and ligands. Some useful information about the effect of polyphenols on the structure of lipase can be obtained by detecting the changes of emission peaks. The intrinsic fluorescence spectra of lipase at λEM=280nm are mainly attributed to tryptophan (Trp), tyrosine (Tyr) and phenylalanine (Phe) in the aromatic ring structure of protein (Cysewski, 2008). The fluorescence emission spectra of lipase in the absence and presence of NCGA and CCGA were measured with 280 nm excitation wavelength. As shown in Fig. 2a1 and 2a2, the fluorescence intensity of lipase decreased gradually with increasing NCGA and CCGA concentrations. Meanwhile, compared to the initial state of the lipase, the relative quenching ratio was approximately equal to 46.48% and 36.71% at the highest concentration of NCGA and CCGA, respectively. These results indicate that NCGA and CCGA can interact with lipase and effectively quench its intrinsic fluorescence. The intrinsic fluorescence of lipase is easily quenched with NCGA, which means there exists more opportunities for the interaction between NCGA and lipase. In addition, the decrease in fluorescence intensity was accompanied by the red shift of the maximum wavelength after the combination of lipase and NCGA which demonstrates a change in the microenvironment of amino acid residues in lipase. A similar result was reported in the binding of CGA with LOX (Cao et al., 2020).

3.2.2 The Fluorescence Quenching Mechanism

In brief, the fluorescence quenching mechanism can be divided into static quenching,

dynamic quenching, or a mixture of both mechanisms (Wang, Kou, Lin, & Shi, 2020; Zhou, Pan, Lou, & Shi, 2018). To further explore the quenching type, Stern-Volmer diagrams in fluorescence quenching of lipase for NCGA and CCGA at two different temperatures (298K (25℃) and 310K (37℃)) were determined (Fig. 2b1 and Fig. 2b2). It can be seen from the curve that the F_0 / F value and the concentration of the quencher show a good linear relationship at different temperatures, which indicates that a pure static or dynamic mechanism appeared in lipase-CCGA and lipase-NCGA interactions (Menezes et al., 2020). The dynamic quenching is the fluorescence quenching caused by the collision between the quencher and the excited state of the fluorescence molecule. The static quenching is the phenomenon that the quencher molecule and the fluorescent material molecule form a non-fluorescence complex at the ground state, which leads to the decrease in fluorescence intensity of the fluorescent material. The slope of the Stern–Volmer plot values decreased gradually with increasing temperatures which provided evidence that the quenching type of lipase fluorescence for NCGA and CCGA was a single static quenching process.

3.2.3 Analysis of the Binding Parameters

The interaction parameters of NCGA and CCGA with lipase at different temperatures are collected in Table 2. The K_q of lipase for NCGA and CCGA were 2.47×10^{12} L/mol·s and 1.5×10^{12} L/mol·s at 298K, respectively, which were much larger than the maximum value of the dynamic quenching rate constant (2.00×10^{10} L / mol · s) in aqueous solution. The results also suggest that the quenching mode of lipase for two polyphenols was a single static quenching (Cui et al., 2015). Both binding site numbers of NCGA and CCGA were found to be close to 1.0, which indicates that there was only one class of binding site for NCGA and CCGA on lipase and the binding molar ratio of 1:1 between both polyphenols and lipase. The n value for NCGA and CCGA combined with

lipase decreased with increasing temperature, which may be due to the decomposition of the lipase-polyphenol complex at higher temperatures.

3.2.4 Measurement of the Thermodynamic Parameters

Calculation of the thermodynamic parameters of the combined reaction helps to determine the main binding force between polyphenols and lipase. In general, there are four types of binding force between small polyphenols and lipase: hydrophobic interaction, hydrogen bond interaction, van der Waals force and electrostatic interaction (Jia, Gao, Hao, & Tang, 2017). As shown in Table 1, the negative values of ΔG indicates that the interaction between chlorogenic acid isomers and lipase occurred spontaneously. For ligand-protein interaction, $\Delta H>0$, $\Delta S>0$ demonstrate hydrophobic interaction; $\Delta H<0$, $\Delta S<0$ signify hydrogen bond and van der Waals interaction; $\Delta H<0$, $\Delta S>0$ imply electrostatic force (Ross & Subramanian, 1981). The negative values of ΔH and ΔS indicate that the binding process of NCGA with endogenous lipase is mainly driven by the hydrogen bond interaction and van der Waals force. The negative value of ΔH and the positive value of ΔS confirm that the electrostatic interaction force may play a major role in the binding process of the lipase-CCGA system.

3.2.5 Synchronous Fluorescence Spectral Measurement

Synchronous fluorescence spectroscopy can provide information about changes in the microenvironment before and after the combination of fluorophore molecules and polyphenols and is an ideal tool for studying protein conformation changes. When the wavelength interval ($\Delta\lambda=\lambda em-\lambda ex$) is set to 15nm and 60nm, the synchronous fluorescence spectrum provides the characteristic information about tyrosine (Tyr) and tryptophan (Trp) residues, respectively (Tang & Zhao, 2019). As shown in Fig. 2c-d, the fluorescence intensities of Tyr and Trp reduced progressively with the

increasing concentration of NCGA and CCGA, which provides evidence for the occurrence of fluorescence quenching during the binding process. Upon addition of NCGA, the maximum emission wavelengths of residue Trp (from 283.40 to 283.00 nm) and residue Tyr (from 294.60 to 293.40 nm) resulted in slight blue shifts of residues (Fig. 2c1 and 2d1), but there was no shift observed for the addition of CCGA (Fig. 2c2 and 2d2).These results imply that the addition of NCGA slightly improved the polarity of the Trp residue microenvironment and somewhat changed the microenvironment near the Tyr residue. The microenvironment of the Tyr residue and Trp residue exhibited no obvious change when CCGA bound to lipase.

It can be seen from Fig. 3a1 and 3a2 that after adding the two chlorogenic acid isomers, the RSFQ value of Tyr was significantly higher than that of Trp, which may indicate that Tyr plays a greater contributing role to the fluorescence quenching effect of lipase.

3.3 UV–VIS spectroscopy analysis

UV-VIS absorption spectroscopy can be used to further explore the actual quenching process and study the changes in the tertiary structure of lipase before and after adding different concentrations of NCGA and CCGA (Shpigelman, Shoham, Israeli-Lev, & Livney, 2014). The UV–VIS absorption spectra of lipase with or without different concentrations of NCGA and CCGA are presented in Fig. 3b1 and 3b2.There are absorption peaks around 275 nm, which can be associated with the $\pi \rightarrow \pi^*$ transition of Phe, Tyr and Trp residues. The increased absorption intensity and red shift of peaks around 275 nm, show that complexes of lipase-NCGA and lipase-CCGA could be formed. The absorbance of lipase-NCGA and lipase-CCGA complexes were significantly elevated with increasing concentrations between 250 nm and 350 nm, demonstrating that NCGA and CCGA could lead to the modification of polarity and hydrophilicity of the microenvironment around

aromatic amino acid residues of lipase. Generally speaking, dynamic quenching only affects the excited state of the fluorophore, the absorption spectrum remains unchanged, while static quenching usually causes the change in the absorption spectrum of the fluorophore (Cui et al., 2015). The absorption spectra of these two types of polyphenol-lipase systems are significantly different from that of lipase alone, and the maximum emission wavelength shifted. These results again confirm that the quenching mechanism is static quenching.

3.4 CD spectra analysis

Circular dichroism is a technique for measuring the conformational changes of proteins, and it is used to study the effect of multiple binding on the secondary structure of lipase (Wu et al., 2018). Fig. 3 c1 and 3c2 display the circular dichroism spectrum of lipase in the absence or presence of polyphenols. The spectra presented two negative bands in the far-UV region at 208 and 222 nm which are typical of the α-helix of protein. With the addition of polyphenols, the negative characteristic peak intensity of lipase decreased, signifying that the secondary structure of lipase has changed. The contents of different secondary structures of lipase are listed in Table S2. Compared to the free lipase, it was obvious that when NCGA and CCGA were added into lipase solutions, the α-helix of polyphenol-lipase complexes increased to 27.4% or 23.10% from the initial 20.40%, respectively. The changes in protein α-helix can be attributed to the fact that the combination of NCGA or CCGA and lipase enhances the degree of contraction of the lipase backbone, which has been reported by other researchers (Tang, Zuo, & Shu, 2014).The analysis result is consistent with the conclusion of the radius of gyration in the molecular dynamics simulation.

3.5 FT-IR spectra studies

The lipase-polyphenol complexes were studied after freeze drying using FTIR to assess the

binding interactions forming the complexes and the influence of the secondary structure of proteins after the addition of small molecules (Zhu et al., 2019). As shown in Fig. 3d1 and 3d2, the FT-IR spectra of lipase and lipase-phenol complex in the range of 4000-400cm^{-1} were studied. The absorption peak of lipase at 3429 cm^{-1} is caused by the N-H and O-H stretching vibrations in the protein molecule, and the newly generated absorption peak at 2927 cm^{-1} is related to the asymmetric stretching vibration of C-H. Amide I band (1700–1600 cm^{-1}, mainly C=O stretching vibration) and amide II band (1600–1500 cm^{-1}, stretching vibration of C-N and the bending vibration of N-H) are the main vibrational bands of the peptide moiety related to the secondary structures of proteins. Amide I bands are more sensitive to changes in the protein secondary structure compared to Amide II bands. It was noticed that the peak positions of the amide I moved from 1648 to 1637 cm^{-1} and 1648 to 1627 cm^{-1}, when NCGA and CCGA were added into lipase solutions, respectively. The peak positions of the amide Ⅱ band shifted from 1540 to 1519 cm^{-1} and 1540 to 1512 cm^{-1} after the addition of NCGA and CCGA respectively. The changes of these peak positions suggest that NCGA and CCGA interacted with both C=O and C-N groups in lipase, which are responsible for changes in the secondary structure of lipase. The findings are in accordance with the CD spectra results.

The results described about CD spectra analysis and FT-IR spectra studies indicate that the combination of polyphenols and polypeptide chains of lipase might have altered the hydrogen bond networks and the secondary structures of the lipase. This in turn might have further hampered enzymatic catalytic sites and active centers, thus, affecting the activity of enzymes.

3.6 Particle size analysis

DLS measurement is to study of the size distribution of lipase and lipase-polyphenol complex, which can provide a qualitative estimate of the protein size and protein aggregation state (Alam et

al., 2017). Fig. 1a2 presents the change in the lipase particle size under different polyphenol concentrations. The average particle size of the lipase added with NCGA ranges from 934.40 ±40.86nm to 1407.00±300.60nm, and that of lipase added with CCGA increased from 934.40±40.86nm to 1222.33±93.77nm. The result illustrates that both NCGA and CCGA can cause lipase aggregation and form lipase-polyphenol complex. Fig. 1d1 and 1d2 shows the molecular weight distribution curve (intensity %), polydispersity index (PDI) and the Z mean values (d.nm) of lipase and the lipase-polyphenol system. The PDI and Z-average of lipase alone were 0.407 and 934.4, respectively. However, after adding polyphenols, the PDI and Z-average values of lipase-NCGA and lipase-CCGA systems increased to 0.581, 1407 and 0.44, 1222.33, respectively. These results suggest that polyphenols can promote the aggregation of lipase and reduce the Dispersion of lipase. These phenomena are also found in the binding between polyphenols and myosin (Huang et al., 2020). It is well known that, PDI values greater than 0.7 represent a very wide size distribution, while PDI values from 0.05 to 0.7 correspond to monodisperse systems (Zhu, Sun, Wang, Xu, & Wang, 2017). As shown in Fig. 1d1 and 1d2, the PDI values of all complexes are lower than 0.4, which implies that the lipase-polyphenol solution meets the monodisperse standard.

3.7 Molecular docking analysis

The molecular docking method was employed to predict the visible binding modes and corresponding mechanism of NCGA-lipase and CCGA-lipase systems. The active site of lipase is composed of serine (Ser), aspartic acid (Asp) and histidine (His) residues and is protected by a helical structure composed of hydrophobic amino acid residues. The best binding site information of the isomer and porcine pancreatic lipase is shown in Fig. 4a-b. Under different conditions, the details of the interaction between amino acid residues and chlorogenic acid

isomers in the three-dimensional docking mode and two-dimensional schematic diagram are illustrated in Fig. 4c-d. The docking result shows that the NCGA forms a hydrogen bond with lipase, including Lys 81 (1.81 Å), Glu 84 (2.31 Å), Arg 257 (2.76 Å) and Asp 80 (1.97 Å), and the carbon-hydrogen bond formed by the oxygen atom on the carboxyl group and His 152 (3.05Å). In addition to hydrogen bonds, the hydrophobic interaction between the benzene ring structure of NCGA and Trp253 (5.11Å) and the weak van der Waals forces around amino acid residues also exist in the interaction (Fig. 4c1). This is consistent with the measurement of thermodynamic parameters. For the lipase-CCGA complex, CCGA forms a hydrogen bond with amino acid residues Asp 80 (2.66 Å) and His 264 (2.39 Å). The hydrophobic interaction also exists between the Trp253 (5.24 Å) and CCGA (Fig. 4c2). The binding site of CCGA and amino acid residues is close to the active site of lipase, which is closely related to enzyme activity.

3.8 Molecular dynamics simulation analysis

Molecular dynamics simulations were carried out to explore the stability of lipase-NCGA and lipase-CCGA complexes. The root mean square deviation (RMSD), root mean square fluctuation (RMSF) and conformational changes in active centers of lipase-NCGA and lipase-CCGA complexes were investigated. The calculation of RMSD can be used to study the trajectory stability of lipase-NCGA and lipase-CCGA complexes, the results are presented in Fig. 5a. After adding CCGA, the RMSD value reached equilibrium after approximately 25 ns simulation time, and oscillated stably around ~0.2 Å, while after the adding NCGA, the RMSD value reached equilibrium after approximately 30 ns simulation time, and fluctuated around 0.3Å, which is larger than the lipase-CCGA system. This evidence clearly shows that the lipase-NCGA and lipase-CCGA complex

systems are both stable and balanced. Compared with the lipase-NCGA system, the lipase-CCGA system has a more stable RMSD value, suggesting that the system is relatively stable. The RMSD value of lipase-NCGA complex is greater than that of lipase-CCGA, which implies that NCGA has a much greater impact on the structural change of lipase. In this study, by calculating the RMSF of the amino acid skeleton atoms of the compound and the receptor protein complex during the molecular dynamics simulation, we analyzed the volatility of the skeleton amino acid during the 75ns-150ns time simulation when lipase interacts with two chlorogenic acid isomers (Fig. 5b). The RMSF value with respect to the simulation time is a tool for evaluating the local conformational changes of lipase. The high fluctuating regions of the lipase-NCGA and lipase-CCGA systems during simulation appeared to have the following residue ranges:100-125, 200-250, 300-350 and 400-425, indicating that NCGA and CCGA can act on the active center of lipase and combine with lipase to form a complex. The radius of gyration is a physical quantity that describes the compactness of a protein， the smaller the radius of gyration, the better the compactness of the protein (Al-Shabib et al., 2020). As it can be seen form Fig. 5 c1 and 5c2, the radius of gyration (Rg) value of lipase in NCGA and CCGA is reduced, which indicates that the structure of lipase becomes more compact after adding NCGA and CCGA, This is consistent with the results of DLS. It was also seen that Rg of lipase in NCGA showed less fluctuation than that of CCGA due to its interactions with different inhibitors.

4 Conclusions

The results suggest that the inhibitory activity of chlorogenic acid isomers (NCGA and CCGA) on lipase is dose dependent and NCGA has stronger inhibitory effect on lipase. The interaction mechanism between NCGA and CCGA and lipase was illuminated by multispectral

technology combined with molecular docking and molecular dynamics simulation. Fluorescence spectroscopy experiment results show that both NCGA and CCGA quench the endogenous fluorescence of lipase through the static quenching style. Compared to the initial state of the lipase, the relative quenching ratio was equal to 46.48% and 36.71% at the highest concentration of NCGA and CCGA, respectively, indicating that NCGA has a greater quenching effect on the lipase. The changes in synchronous fluorescence spectroscopy showed that the microenvironment of lipase greatly changed after NCGA was added. The results of ultraviolet absorption spectroscopy established that the new complexes were formed between lipase and NCGA and CCGA. CD spectra and FT-IR spectra confirmed the alteration of the lipase secondary structure. DLS results demonstrated that NCGA and CCGA can promote the accumulation of lipase. Molecular docking indicates that the main binding force between NCGA and lipase is hydrogen bond and van der Waals force. In addition, the thermodynamic functions ΔH and ΔS are -228.56KJ/mol and -665.54 J/mol·K, signifying that hydrogen bond and van der Waals force are the main acting forces between NCGA and lipase. The molecular dynamics simulations analysis showed that NCGA has a greater impact on the structure of lipase and binds more closely to the lipase and the addition of chlorogenic acid isomers made the lipase structure more compact.

Credit authorship contribution statement

Zeru Xu: Methodology, Formal analysis, Writing – original draft. **Qiongju Cao:** Methodology, Formal analysis. **Shanbai Xiong:** Project administration. **Anne Manyande:** Writing - review & editing. **Hongying Du:** Supervision, Conceptualization, Formal analysis, Funding acquisition, Writing - review & editing.

Acknowledgments

This research was financially supported by the Fundamental Research Funds for the Central

Universities of China (No. 2662019PY031), the National Natural Science Foundation of China (No. 31772047) and the National Key R & D Program of China (No. 2019YFC1606003).

Conflict of Interest

The authors have no conflict of interest.

References

Al-Shabib, N. A., Khan, J. M., Malik, A., Tabish Rehman, M., AlAjmi, M. F., Husain, F. M., . . . Altwaijry, N. (2020). Molecular interaction of tea catechin with bovine β-lactoglobulin: A spectroscopic and in silico studies. *Saudi Pharmaceutical Journal, 28*(3), 238-245. doi: https://doi.org/10.1016/j.jsps.2020.01.002

Alam, P., Beg, A. Z., Siddiqi, M. K., Chaturvedi, S. K., Rajpoot, R. K., Ajmal, M. R., . . . Khan, R. H. (2017). Ascorbic acid inhibits human insulin aggregation and protects against amyloid induced cytotoxicity. *Archives of Biochemistry and Biophysics, 621*, 54-62. doi: https://doi.org/10.1016/j.abb.2017.04.005

Bu, T., Jin, Y., Li, X., Zhang, J., Xu, D., Yang, W., & Lou, Q. (2017). Effect of electron irradiation and bayberry polyphenols on the quality change of yellowfin tuna fillets during refrigerated storage. *Radiation Physics and Chemistry, 138*, 67-71. doi: https://doi.org/10.1016/j.radphyschem.2017.03.025

Cao, Q., Du, H., Huang, Y., Hu, Y., You, J., Liu, R., . . . Manyande, A. (2019). The inhibitory effect of chlorogenic acid on lipid oxidation of grass carp (Ctenopharyngodon idellus) during chilled storage. *Food and Bioprocess Technology, 12*(12), 2050-2061. doi: 10.1007/s11947-019-02365-0

Cao, Q., Huang, Y., Zhu, Q.-F., Song, M., Xiong, S., Manyande, A., & Du, H. (2020). The mechanism of chlorogenic acid inhibits lipid oxidation: An investigation using multi-spectroscopic methods and molecular docking. *Food Chemistry, 333*, 127528. doi: https://doi.org/10.1016/j.foodchem.2020.127528

Chaijan, S., Panpipat, W., Panya, A., Cheong, L.-Z., & Chaijan, M. (2020). Preservation of chilled Asian sea bass (Lates calcarifer) steak by whey protein isolate coating containing polyphenol extract from ginger, lemongrass, or green tea. *Food Control, 118*, 107400. doi: https://doi.org/10.1016/j.foodcont.2020.107400

Cherif, S., & Gargouri, Y. (2009). Thermoactivity and effects of organic solvents on digestive lipase from hepatopancreas of the green crab. *Food Chemistry, 116*(1), 82-86. doi: https://doi.org/10.1016/j.foodchem.2009.02.009

Cieplak, P., Cornell, W., Bayly, C., & Kollman, P. (1995). Application of the Multimolecule and Multiconformational RESP Methodology to Biopolymers - Charge Derivation for DNA, RNA, and Proteins. *Journal of Computational Chemistry, 16*, 1357-1377. doi: 10.1002/jcc.540161106

Cui, Y., Liang, G., Hu, Y. H., Shi, Y., Cai, Y. X., Gao, H. J., . . . Wang, Q. (2015). Alpha-substituted derivatives of cinnamaldehyde as tyrosinase inhibitors: inhibitory mechanism and molecular analysis. *J Agric Food Chem, 63*(2), 716-722. doi: 10.1021/jf505469k

Cysewski, P. (2008). A post-SCF complete basis set study on the recognition patterns of uracil and cytosine by aromatic and π-aromatic stacking interactions with amino acid residues. *Physical chemistry chemical physics : PCCP, 10*, 2636-2645. doi: 10.1039/b718394a

Huang, X., & Ahn, D. U. (2019). Lipid oxidation and its implications to meat quality and human health. *Food Science and Biotechnology, 28*(5), 1275-1285. doi: 10.1007/s10068-019-00631-7

Huang, Y., Du, H., Kamal, G. M., Cao, Q., Liu, C., Xiong, S., . . . Huang, Q. (2020). Studies on the Binding Interactions of Grass Carp (Ctenopharyngodon idella) Myosin with Chlorogenic Acid and Rosmarinic Acid. *Food and Bioprocess Technology, 13*(8), 1421-1434. doi: 10.1007/s11947-020-02483-0

Jia, J., Gao, X., Hao, M., & Tang, L. (2017). Comparison of binding interaction between β-lactoglobulin and three common polyphenols using multi-spectroscopy and modeling methods. *Food Chemistry, 228*, 143-151. doi: https://doi.org/10.1016/j.foodchem.2017.01.131

Ju, J., Liao, L., Qiao, Y., Xiong, G., Li, D., Wang, C., . . . Li, X. (2018). The effects of vacuum package combined with tea polyphenols (V+TP) treatment on quality enhancement of weever (Micropterus salmoides) stored at 0 °C and 4 °C. *LWT, 91*, 484-490. doi: 10.1016/j.lwt.2018.01.056

Khoury, G. A., Bhatia, N., & Floudas, C. A. (2014). Hydration free energies calculated using the AMBER ff03 charge model for natural and unnatural amino acids and multiple water models. *Computers & Chemical Engineering, 71*, 745-752. doi: https://doi.org/10.1016/j.compchemeng.2014.07.017

Kuepethkaew, S., Sangkharak, K., Benjakul, S., & Klomklao, S. (2017). Use of TPP and ATPS for partitioning and recovery of lipase from Pacific white shrimp (Litopenaeus vannamei) hepatopancreas. *Journal of Food Science and Technology, 54*(12), 3880-3891. doi: 10.1007/s13197-017-2844-9

Maqsood, S., Benjakul, S., & Shahidi, F. (2013). Emerging Role of Phenolic Compounds as Natural Food Additives in Fish and Fish Products. *Critical Reviews in Food Science and Nutrition, 53*(2), 162-179. doi: 10.1080/10408398.2010.518775

Martínez-González, A., Alvarez-Parrilla, E., Díaz-Sánchez, Á., De la Rosa, L., Núñez-Gastélum, J. A., Vazquez-Flores, A., & Aguilar, G. (2017). In Vitro Inhibition of Pancreatic Lipase by Polyphenols: A Kinetic, Fluorescence Spectroscopy and Molecular Docking Study. *Food Technology and Biotechnology, 55*. doi: 10.17113/ftb.55.04.17.5138

Menezes, T. M., Barros, M. R., Ventura, G. T., de Sa Pires Ferreira, D., Todeschini, A. R., Borges, R. M., . . . Neves, J. L. (2020). Insights on the interaction of furfural derivatives with BSA and HTF by applying multi-spectroscopic and molecular docking approaches. *Journal of Molecular Liquids, 317*, 114021. doi: https://doi.org/10.1016/j.molliq.2020.114021

Olatunde, O. O., & Benjakul, S. (2018). Natural Preservatives for Extending the Shelf-Life of Seafood: A Revisit. *Comprehensive Reviews in Food Science and Food Safety, 17*(6), 1595-1612. doi: https://doi.org/10.1111/1541-4337.12390

Ross, P., & Subramanian, S. (1981). Thermodynamics of Protein Association Reactions - Forces Contributing to Stability. *Biochemistry, 20*, 3096-3102. doi: 10.1021/bi00514a017

Secci, G., & Parisi, G. (2016). From farm to fork: lipid oxidation in fish products. A review. *Italian Journal of Animal Science, 15*(1), 124-136. doi: 10.1080/1828051X.2015.1128687

Shpigelman, A., Shoham, Y., Israeli-Lev, G., & Livney, Y. D. (2014). β-Lactoglobulin–naringenin complexes: Nano-vehicles for the delivery of a hydrophobic nutraceutical. *Food Hydrocolloids, 40*, 214-224. doi: https://doi.org/10.1016/j.foodhyd.2014.02.023

Siscovick David, S., Barringer Thomas, A., Fretts Amanda, M., Wu Jason, H. Y., Lichtenstein Alice, H., Costello Rebecca, B., . . . Mozaffarian, D. (2017). Omega-3 Polyunsaturated Fatty Acid (Fish Oil) Supplementation and the Prevention of Clinical Cardiovascular Disease. *Circulation, 135*(15), e867-e884. doi: 10.1161/CIR.0000000000000482

Smichi, N., Gargouri, Y., Miled, N., & Fendri, A. (2013). A grey mullet enzyme displaying both lipase and phospholipase activities: Purification and characterization. *International Journal of Biological Macromolecules, 58*, 87-94. doi: https://doi.org/10.1016/j.ijbiomac.2013.03.056

Tang, H., & Zhao, D. (2019). Investigation of the interaction between salvianolic acid C and xanthine oxidase: Insights from experimental studies merging with molecular docking methods. *Bioorganic Chemistry, 88*, 102981. doi: https://doi.org/10.1016/j.bioorg.2019.102981

Tang, L., Zuo, H., & Shu, L. (2014). Comparison of the interaction between three anthocyanins and human serum albumins by spectroscopy. *Journal of Luminescence, 153*, 54-63. doi: https://doi.org/10.1016/j.jlumin.2014.03.004

Wang, B.-L., Kou, S.-B., Lin, Z.-Y., & Shi, J.-H. (2019). Investigation on the binding behavior between BSA and lenvatinib with the help of various spectroscopic and in silico methods. *Journal of Molecular Structure, 1204*, 127521. doi: 10.1016/j.molstruc.2019.127521

Wang, B.-L., Kou, S.-B., Lin, Z.-Y., & Shi, J.-H. (2020). Investigation on the binding behavior between BSA and lenvatinib with the help of various spectroscopic and in silico methods. *Journal of Molecular Structure, 1204*, 127521. doi: https://doi.org/10.1016/j.molstruc.2019.127521

Wei, P., Zhu, K., Cao, J., Dong, Y., Li, M., Shen, X., . . . Li, C. (2021). The inhibition mechanism of the texture deterioration of tilapia fillets during partial freezing after treatment with polyphenols. *Food Chemistry, 335*, 127647. doi: https://doi.org/10.1016/j.foodchem.2020.127647

Wu, H., Zeng, W., Chen, L., Yu, B., Guo, Y., Chen, G., & Liang, Z. (2018). Integrated multi-spectroscopic and molecular docking techniques to probe the interaction mechanism between maltase and 1-deoxynojirimycin, an α-glucosidase inhibitor. *International Journal of Biological Macromolecules, 114*, 1194-1202. doi: https://doi.org/10.1016/j.ijbiomac.2018.04.024

Yerlikaya, P., & Gokoglu, N. (2010). Inhibition effects of green tea and grape seed extracts on lipid oxidation in bonito fillets during frozen storage. *International Journal of Food Science & Technology, 45*(2), 252-257. doi: https://doi.org/10.1111/j.1365-2621.2009.02128.x

Yu, Q., Fan, L., & Duan, Z. (2019). Five individual polyphenols as tyrosinase inhibitors: Inhibitory activity, synergistic effect, action mechanism, and molecular docking. *Food Chemistry, 297*, 124910. doi: https://doi.org/10.1016/j.foodchem.2019.05.184

Zhang, C., Zhang, G., Pan, J., & Gong, D. (2016). Galangin competitively inhibits xanthine oxidase by a ping-pong mechanism. *Food Research International, 89*, 152-160. doi: https://doi.org/10.1016/j.foodres.2016.07.021

Zhou, K.-L., Pan, D.-Q., Lou, Y.-Y., & Shi, J.-H. (2018). Intermolecular interaction of fosinopril with bovine serum albumin (BSA): The multi-spectroscopic and computational investigation. *Journal of Molecular Recognition, 31*, e2716. doi: 10.1002/jmr.2716

Zhu, J., Sun, X., Wang, S., Xu, Y., & Wang, D. (2017). Formation of nanocomplexes comprising whey proteins and fucoxanthin: Characterization, spectroscopic analysis, and molecular docking. *Food Hydrocolloids, 63*, 391-403. doi: https://doi.org/10.1016/j.foodhyd.2016.09.027

Zhu, S., Yuan, Q., Yang, M., You, J., Yin, T., Gu, Z., . . . Xiong, S. (2019). A quantitative comparable study on multi-hierarchy conformation of acid and pepsin-solubilized collagens from the skin of grass carp (Ctenopharyngodon idella). *Materials Science and Engineering: C, 96*, 446-457. doi: https://doi.org/10.1016/j.msec.2018.11.043

Table 1. Quenching constant (K_{SV}), binding constant (K_a) and thermodynamic parameters of lipase-NCGA and lipase-CCGA at different temperatures

	T (K)	K_{sv} (10^4 L/mol)	K_q (10^{12} L/mol·s)	R_a^2	K_a (10^5 L/mol)	n	R_b^2	ΔH (KJ/mol)	ΔS (J/mol·K)	ΔG (KJ/mol)
NCGA	298	2.47	2.47	0.994	1.98	1.20	0.993			-30.23
	310	2.08	2.08	0.993	0.06	0.87	0.986	-228.56	-665.54	-22.24
CCGA	298	1.50	1.50	0.985	5.74	1.36	0.983			-32.85
	310	1.31	1.31	0.972	5.27	1.36	0.995	-5.41	92.09	-33.96

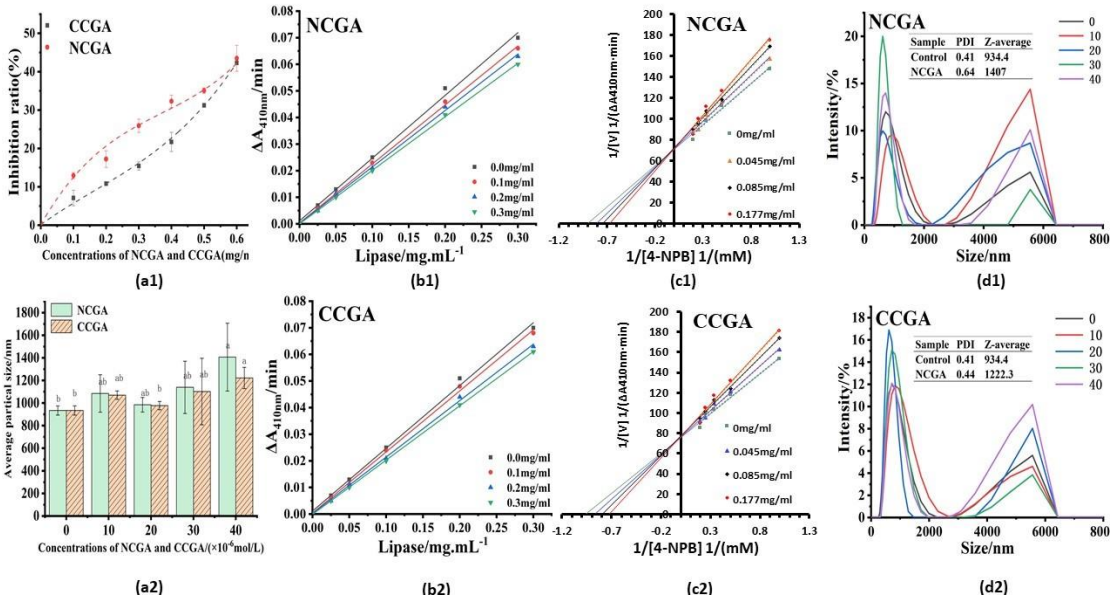

Fig. 1. Inhibition ratio of NCGA and CCGA to lipase (a1) and particle size analysis (a2 d1 d2). Types of inhibition of lipase for NCGA(b1) and CCGA(b2). The inhibition kinetics of NCGA(c1) and CCGA(c2) on lipase.

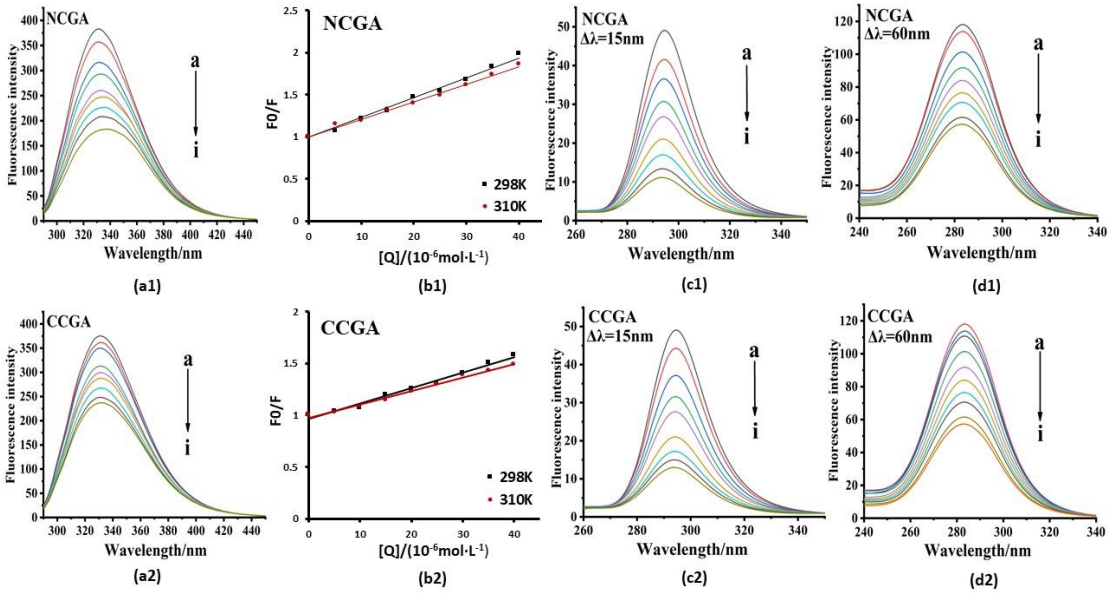

Fig. 2. Fluorescence spectra analysis of the interaction between lipase and NCGA (a1-d1) or CCGA (a2-d2). Changes in the intrinsic fluorescence of lipase without or with different concentrations of NCGA (a1) and CCGA (a2) at 298K. The Stern-Volmer plots for the quenching of lipase for NCGA (b1) and CCGA (b2) in 298 K and 310 K. Synchronous fluorescence spectra of the interaction between lipase and NCGA (c)/CCGA(d) at $\Delta\lambda$ = 15 nm (c1 and c2) and at $\Delta\lambda$ = 60 nm (d1, and d2); the concentrations of NCGA and CCGA were 0.00 to 40.00×10^{-6}mol/L with a concentration gradient of 5×10^{-6}mol/L for curves a→i, respectively.

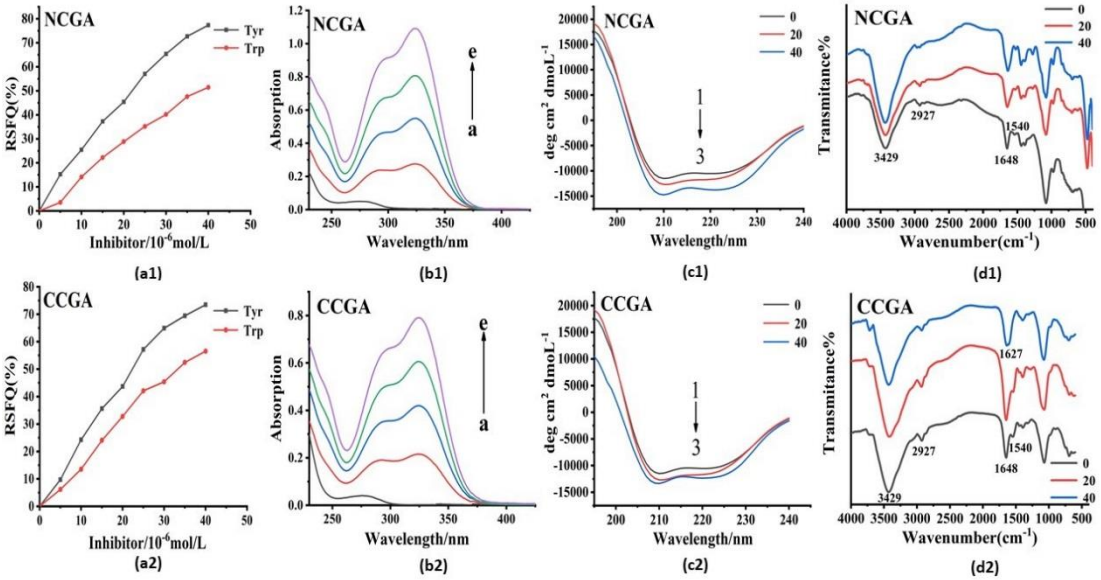

Fig. 3. UV–VIS、FT-IR and CD spectra and RSFQ analysis of lipase after the interaction of NCGA(a1-d1) and CCGA(a2-d2). CD spectra of lipase in the absence and presence of NCGA (c1) and CCGA (c2), the concentrations of NCGA and CCGA were 0.00, 20.00,40.00×10^{-6}mol/L for curves 1→3, respectively. UV–VIS spectra of lipase with various concentrations of NCGA (b1 a →e=0,10,20,30,40×10^{-6}mol/L) and CCGA (b2 a→e=0,10,20,30,40×10^{-6} mol/L).

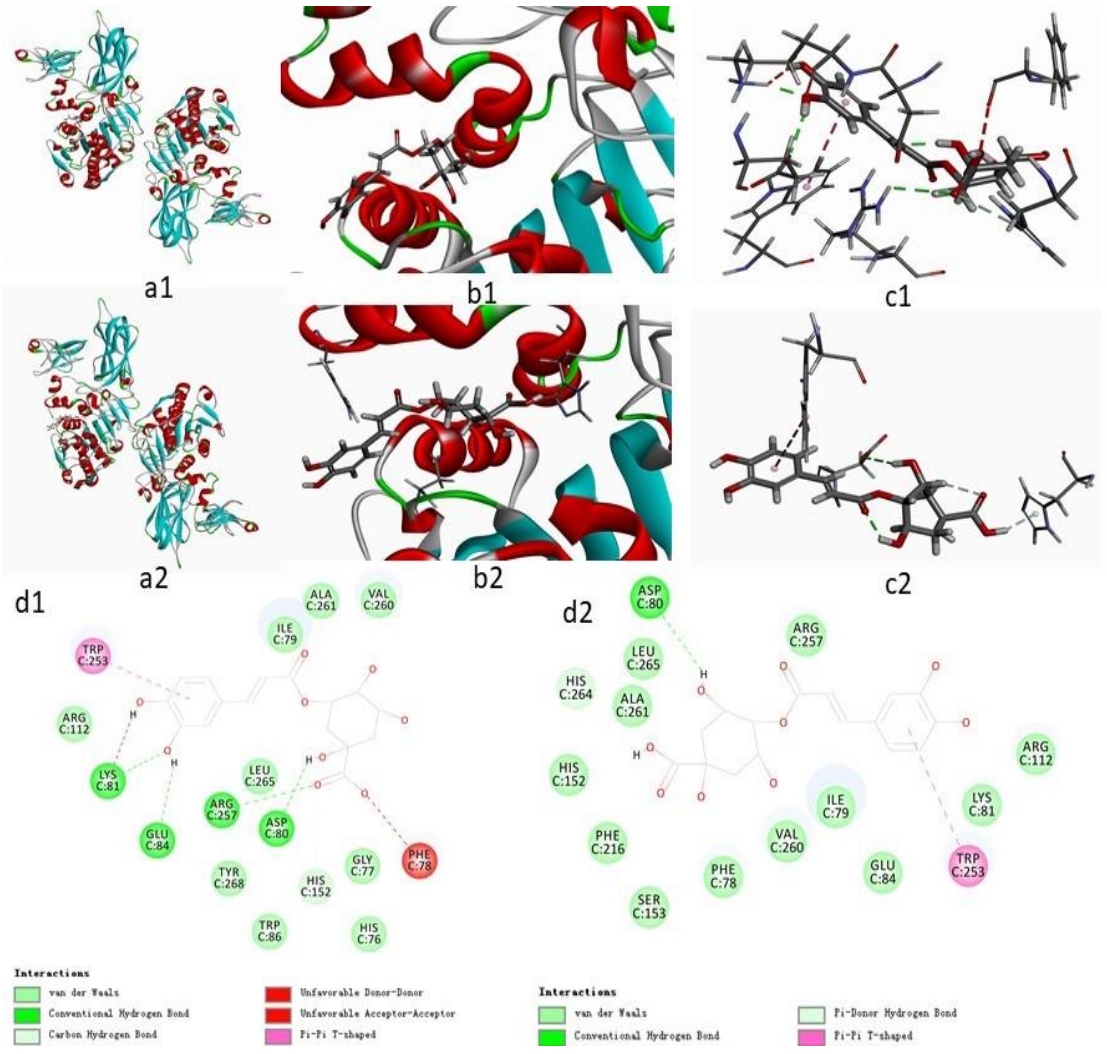

Fig. 4. Molecular docking analysis of the interaction of lipase and NCGA (a1-d1) or CCGA (a2-d2).

Note: a) and b): Docking ligand at the binding site; c) Results of 3D molecular docking modeling; d) Results of 2D molecular docking modeling.

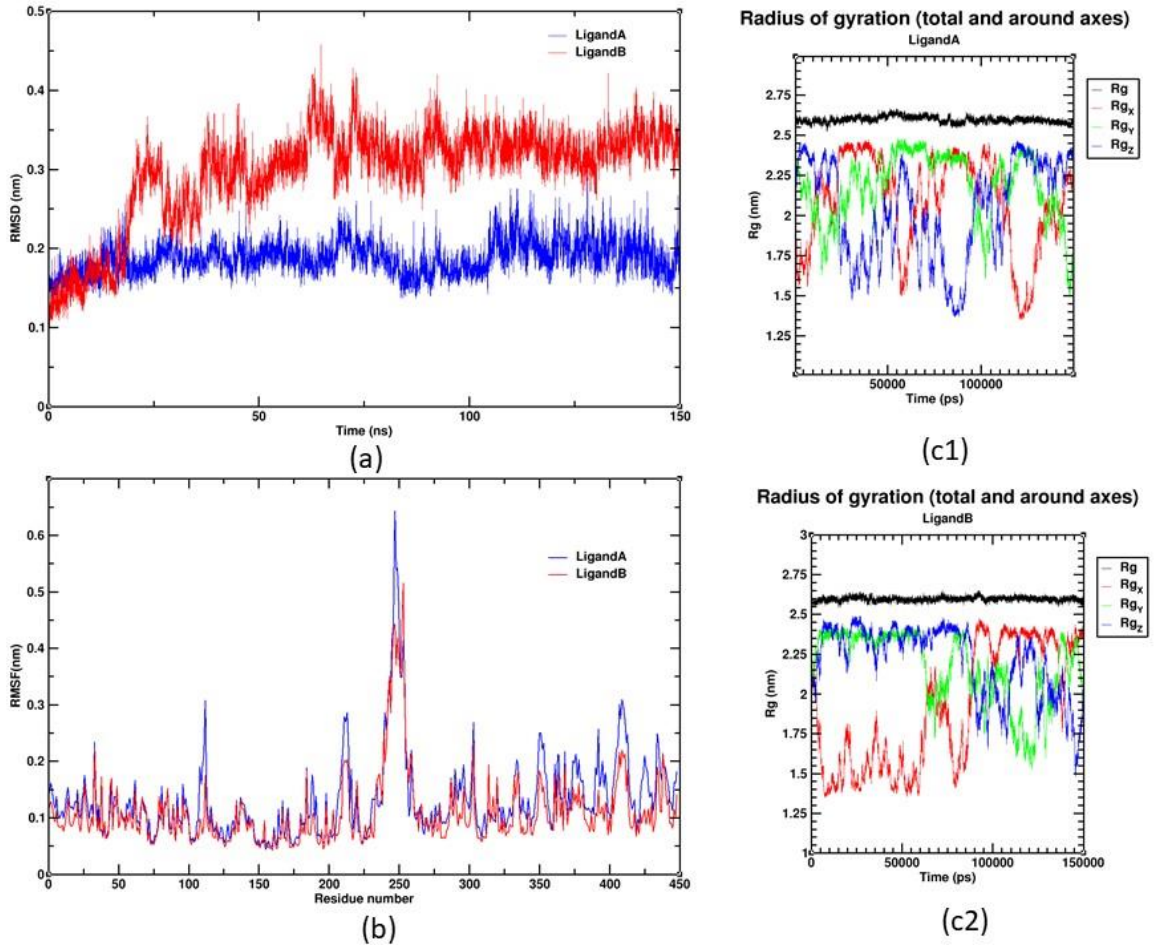

Fig. 5. Profiles of molecular dynamics simulations: (a) RMSD values for NCGA-lipase complexes (red) and CCGA-lipase complexes (blue); (b). The RMSF values of NCGA-lipase complexes (red) and CCGA-lipase complexes (blue); (c1 c2). Time evolution of the radius of gyration (Rg) during 150 ns of MD simulation of NCGA-lipase complex (c2) and CCGA-lipase complex (c1)